International Journal of Pharmaceutics 414 (2011) 251–259

Contents lists available at ScienceDirect

International Journal of Pharmaceutics

journal homepage: www.elsevier.com/locate/ijpharm

Pharmaceutical Nanotechnology

# Characterization, pharmacokinetics and disposition of novel nanoscale preparations of paclitaxel

Cheng Wang, YingJing Wang, YuJun Wang, Min Fan, Feng Luo, ZhiYong Qian*

*State Key Laboratory of Biotherapy and Cancer Center, West China Hospital, West China Medical School, Sichuan University, Chengdu 610041, China*

ARTICLE INFO

*Article history:*
Received 18 March 2011
Received in revised form 19 April 2011
Accepted 1 May 2011
Available online 10 May 2011

*Keywords:*
Polymeric nanoparticle
Paclitaxel
Amphiphilic diblock copolymer
MPEG–PCL
Solid dispersion technique

ABSTRACT

Polymeric nanoparticles (NPs) have great potential application in achieving targeted delivery of anticancer drugs. Paclitaxel (PTX) loaded NPs were developed using biodegradable methoxy poly (ethylene glycol)–poly ($\varepsilon$-caprolactone) (MPEG–PCL) diblock copolymer by solid dispersion technique without toxic organic solvent. The lyophilized powder has been stored at room temperature for more than six months and still unchanged. PTX-loaded MPEG–PCL nanoparticles (PTX-NPs) displayed that the highest drug loading of PTX was about 25.6% and entrapment efficiency was over 98%, and the optimized average diameter and polydispersity index (PDI) were about 27.6 ± 0.1 nm and 0.05, respectively. Moreover, experimental results shown PTX-NPs had sustained-release effects and its curve fitting followed the Higuchi model. The maximum tolerated dose (MTD) of PTX-NPs after single dose in Balb/c mice was above 80 mg PTX/kg body weight (b.w), which was 2.6-fold higher than that of Taxol® (30 mg PTX/kg b.w). The levels of PTX administrated PTX-NPs had obvious distinction to Taxol® in plasma, liver, spleen, kidneys, lungs, heart and tumor. Especially, the concentration of PTX in tumor administrated PTX-NPs was higher than administration of Taxol®. All results suggested that we had contrived a simple, biodegradable, effective and controllable drug delivery system for paclitaxel.



## 1. Introduction

Due to poor water solubility of many therapeutic compounds, their applications to clinical research were greatly restricted. Paclitaxel (PTX) is a natural anticancer drug, which is effective in treating ovarian cancer, breast cancer, stomach cancer, lung cancer, thyroid cancer, non-small cell lung cancer, AIDS related Kaposi's sarcoma, etc. (Wall, 1998). However, because of its poor aqueous solubility and low therapeutic index, the clinical applications are extremely limited. Clinical applications of PTX (Taxol®) are usually formulated based on Cremophor EL (527 mg/mL) and ethanol (Vyas and Vittorio, 1995). Unfortunately, serious side effects are associated with alcohol-based solvents and Cremophor EL, such as severe hypersensitivity reactions (Weiss et al., 1990), peripheral neuropathy (Rowinsky et al., 1993), etc., which are not well tolerated for patients (Terwogt et al., 1997).

To date, numerous techniques have been attempted to improve the solubility of PTX, such as self-emulsion (Chu et al., 2009), inclusion compound (Liu et al., 2003; Yigitbasi et al., 2004; Zhang et al., 2005), liposomes (Wu et al., 2006), nanosphere (Gao et al., 2008; Gaucher et al., 2010; Hammady et al., 2009; Miglietta et al., 2000; Mu et al., 2010; Musumeci et al., 2006; Ravi Kumar et al., 2004; Wang et al., 2007; Zhang et al., 1996), nanoparticles (Dong and Feng, 2004; He et al., 2007; Lee et al., 2008; Li et al., 2008; Önyüksel et al., 2009; Yadav et al., 2007; Zhang et al., 2005), etc. Polymeric nanoparticle (NP) is a very promising drug delivery system, which has attracted many researchers' attention. Many papers about copolymer nanoparticles have been published (Chan et al., 2009; Gao et al., 2008; Gaucher et al., 2010; Kim et al., 2001; Matsumura, 2008; Mu et al., 2010; Wang et al., 2007; Zhang et al., 1996), only a limited number of products have been successfully used in clinical research (Kim et al., 2001; Matsumura, 2008). The reasons, apart from the toxicity and cost of materials, ascribe to be that many new technologies or concepts were within academia and were not suitable for scaling up.

Now the greatest challenge in developing cancer drugs is to deliver them to the target tumor tissues with lower systemic toxicity. Because tumor tissues have abnormal blood vessels with large pores, NPs in the range of 10–100 nm can leak into the surrounding tumor tissue, which was known as enhanced permeability and retention (EPR) effect (Maeda et al., 2000). It allowed NPs to passively accumulate in the tumor to reduce the side effects of cancer drugs.

Amphiphilic block copolymers are composed of hydrophobic and hydrophilic segments. In aqueous solution, they can self-assemble to form core-shell micellar nanostructures with hydrophobic segments (core) serving as the nanocontainer of

* Corresponding author. Tel.: +86 28 85164063; fax: +86 28 85164060.
*E-mail address:* anderson-qian@163.com (Z. Qian).

0378-5173/$ – see front matter © 2011 Elsevier B.V. All rights reserved.
doi:10.1016/j.ijpharm.2011.05.014

hydrophobic compounds and hydrophilic domain (shell) serving as a stabilizing interface of NPs. The size of polymeric micelle is typically in range of 10–100 nm. So far, various preparation approaches such as dialysis (Cha et al., 2009; Gong et al., 2009; Letchford et al., 2009; Sheikh et al., 2009), oil-in-water (Jaromin et al., 2006), solvent evaporation (Chavanpatil et al., 2006; Jackson et al., 2004; Jin et al., 2007; Li et al., 2009; Mo and Lim, 2005; Westedt et al., 2007), co-solvent evaporation (Jette et al., 2004; Misra et al., 2009), freeze-drying method (Fournier et al., 2004), and etc., have been developed. However, many current papers focus exclusively on studies of pharmacy stability (clarify or precipitation), while ignoring the preparation process, especially the chemical stability of drugs or using many toxic organic solvents during the preparation process, these factors led to its difficulty to promote the use of existing technology. Therefore, in the future researchers should pay more attention to the preparation process of NPs. With the development of nanoscience, many hurdles of drug formulations can be overcome in the future.

In present work, the MPEG–PCL diblock copolymers shows a wonderful combination with PTX. This PTX-loaded MPEG–PCL nanoparticles (PTX-NPs) and preparation technology are better than PTX formulations previously reported (Beletsi et al., 2008; Chang and Chu, 2008; Dong et al., 2010; Dong and Feng, 2004, 2007; Duan et al., 2006; Gryparis et al., 2007; Katsikogianni and Avgoustakis, 2006; Kim and Lee, 2001; Ko et al., 2007; Lee et al., 2008; Ngawhirunpat et al., 2009; van Hasselt et al., 2009; Wu et al., 2006; Xiong et al., 2008; Zhang et al., 2005). The PTX-NPs was prepared through solid dispersion technique without organic solvent, and the lyophilized powder without cryoprotector can be easily redispersed in water. PTX-NPs may be an excellent PTX formulation that may enter market in the future.

## 2. Materials and methods

### 2.1. Materials

Monomethoxy poly(ethylene glycol) (MPEG, *Mn* = 750, 2000, and 5000, Aldrich, USA), $\varepsilon$-caprolactone ($\varepsilon$-CL, Alfa Aesar, USA), stannous octoate ($Sn(Oct)_2$), Dulbecco's modified Eagle's medium (DMEM), 3-(4,5-dimethylthiazol-2-yl)-2,5-diphenyl tetrazolium bromide (MTT) and Paclitaxel were purchased from Sigma (USA). Dehydrated alcohol, dimethylformamide (DMF), tert-butyl alcohol, dichloromethane (DCM) and petroleum ether were purchased from Kelong Chemicals (Chengdu, China). TAXOL® (Bristol-Myers Squibb, USP). The animals were purchased from the Laboratory Animal Center of Sichuan University (Chengdu, China). The animals were housed at temperature of 20–22 °C, relative humidity of 50–60% and 12 h light-dark cycles. Free access to food and water was allowed. All animals would be in quarantine for a week before treatment. All animals care and experimental procedures were conducted according to Institutional Animal Care and Use guidelines.

### 2.2. Methods

#### 2.2.1. Synthesis of diblock copolymer

MPEG–PCL copolymers with different molecular weight ratios of MPEG/PCL were synthesized by ring-opening polymerization according to previous report (Wei et al., 2009). The obtained MPEG–PCL copolymers were purified and kept in air-tight bags before further application. The macromolecular weight (*Mn*) was characterized by proton nuclear magnetic resonance ($^1$H NMR) spectroscopy.

#### 2.2.2. Preparation of PTX-NPs

*2.2.2.1. Preparation of PTX-NPs with different Mn ratios of MPEG–PCL.* At 40 °C, ninety-two milligrams of MPEG–PCL copolymer with different macromolecular weights and eight milligrams of PTX were dissolved in 3 ml of dehydrated alcohol under vigorous stirring. After all contents were dissolved, the solution was evaporated on a rotary evaporator under reduced pressure at 60 °C. When alcohol was evaporated, homogenous coevaporation was obtained. PTX was distributed in polymeric carriers as amorphous form. Then the coevaporation was dissolved in water at 65 °C to create PTX-NPs solution, and the solution was filtered with a 0.22 μm filter to gain a clarified solution. Then the solution was lyophilized in a freeze dry system to receive dried PTX-NPs powder.

*2.2.2.2. Preparation of PTX-NPs with different methods. (1) Dialysis method.* PTX-NPs were prepared according to the method reported previously (Kim and Lee, 2001): PTX (8 mg) and MPEG–PCL (92 mg) were dissolved in 10 ml DMF. Then the solution was transferred into a dialysis tube (Spectrapore, MWCO3500) to dialyze against distilled water for 24 h. The outer solution was exchanged at appropriate time interval. After 4000 r/min centrifuged, the supernatant solution was filtered with a 0.22 μm filter to gain a clarified solution and then freeze-dried to obtain the resultant drug-loaded powder. The dried powder was rehydrated with water before application.

*(2) Solid dispersion technique.* The process for the preparation of PTX-NPs was the same as the method of preparation of PTX-NPs with different *Mn* ratios of MPEG–PCL.

*(3) Freeze-drying* PTX (8 mg) and MPEG–PCL (92 mg) were dissolved in 4 ml tert-butyl alcohol (TBA)/water (v/v, 3:1) mixed solution. The solution was filtered with a 0.22 μm filter to gain a clarified solution and then freeze-dried. The dried power was rehydrated with water before application (Fournier et al., 2004).

#### 2.2.3. Characterization of PTX-NPs

*2.2.3.1. Drug loading, entrapment efficiency and yield.* The amount of nanoparticles was first dissolved in acetonitrile to destruct its package status and filtered through 0.22 μm filter to obtain a clear solution, then the sample solution was determined at 227 nm using reverse-phase High Performance Liquid Chromatography (RP-HPLC) with a $C_{18}$ column (4.6 mm × 150 mm – 5 μm, Grace Analysis column), with acetonitrile/water (48/52, v/v) as eluent solution. Drug-loading (DL), entrapment efficiency (EE) and yield (Y) were obtained by the following calculation equations:

$$\text{DL}\ \% = \frac{\text{Amount of PTX determined in micelle}}{\text{Amount of PTX determined} + \text{copolymer}} \times 100\% \quad (1)$$

$$\text{EE}\ \% = \frac{\text{Amount of PTX loaded in micelle}}{\text{Amount of PTX in feed}} \times 100\% \quad (2)$$

$$\text{Y}\ \% = \frac{\text{Amount of freeze-dried powder}}{\text{Amount of PTX and copolymer in feed}} \times 100\% \quad (3)$$

The characterization of PTX-NPs such as particle size, zeta potential and polydispersity index (PDI) were characterized by Malvern Nano-ZS 90 laser particle size analyzer after equilibration for 10 min. The stability of the NPs was evaluated based on the *Particulate Matter in injections* of USP Pharmacopoeia, each sample should be inspected without observable foreign and particulate matter in its solution. The morphological characteristics of PTX-NPs were examined by transmission electron microscope (TEM, H-6009IV, Hitachi, Japan): nanoparticles were diluted with distilled water and placed on a copper grid covered with nitrocellulose. The samples were negatively stained with phosphotungstic acid and dried at room temperature.

*2.2.3.2. Crystallographic study.* Crystallographic assay was performed on PTX powder, blank MPEG–PCL copolymer, physical mixture of PTX and MPEG–PCL, and PTX-NPs freeze-dried powder by PHILIPS X-ray Diffraction (XRD, X'Pert Pro, MPDDY 1291) using

Cu $K_\alpha$ radiation. Samples were scanned from 5° to 40° at a scanning speed of 1°/min and a step size of 0.05° $2\theta$. The X-ray tube was operated at a potential of 40 kV and a current of 35 mA.

*2.2.4. In vitro drug release behavior*

*In vitro* release behavior of PTX from PTX-NPs was developed by dialysis method, which was shown as follows: 1 ml of reconstituted PTX-NPs freeze-dried powder with water (equal to 1.0 mg of PTX) and 1.0 ml of PTX solution in DMSO (1 mg/ml) were placed in dialysis bags (molecular mass cut off is 8–14 kDa). The dialysis bags were incubated in 40 ml of phosphate buffer (pH = 7.4) containing Tween80 (0.5%, w/v) at 37 °C with 100 r/min stirring, 2 ml of medium was drawn and replaced by fresh incubation medium at predetermined time points. The sample solution was centrifuged with 6000 r/min for 10 min to get supernatant. The drug in supernatant was quantified by the same method of DL. All results were the mean of three test runs, and all data were expressed as the mean ± S.D.

*2.2.5. Cell viability assay*

*In vitro* cytotoxicity of the drugs was determined by standard MTT assays using murine breast cancer cell 4T1. In addition, the cytotoxicity of blank copolymer material was also tested using human embryonic kidney 293 cells (HEK293) and L929 cells. Primarily, cells were plated at a density of $1 \times 10^4$ cells per well in 100 μl of DMEM medium in 96-well plates and grown for 24 h. The cells were then exposed to a series of different concentrations of blank polymeric material, free PTX, Taxol® and PTX-NPs for 48 h. After that, 20 μl MTT solution (5 mg/ml) was added to each well and the plates were continue incubated for another 4 h, allowing the viable cells to transform the yellow MTT into dark-blue formazan crystals, which were dissolved in 160 μl of dimethyl sulphoxide (DMSO). The optical density (OD) of each well was measured at 570 nm by an ELISA microplate reader (ELX800 Biotek, USA), respectively. Cell viability (CV) was determined by the following formula:

$$\text{CV}\ (\%) = \frac{\text{OD(test well)}}{\text{OD(reference well)}} \times 100\% \quad (4)$$

All the results obtained from MTT assays were confirmed by repeating at six individual experiments, and all data were expressed as the mean ± S.D.

*2.2.6. In vitro hemolytic test*

*In vitro* hemolytic study of PTX-NPs was performed. Briefly, 2.5 ml of blank MPEG–PCL polymer (50 mg/ml) and 2.5 ml of PTX-NPs (0.4 mg/ml, obtained from the maximum recommended therapeutic dose for human), 0.8 mg/ml, 1.0 mg/ml, 1.6 mg/ml of PTX in normal saline were added into 2.5 ml of rabbit erythrocyte suspension (2%) in normal saline at 37 °C. Normal saline and distilled water were employed as negative and positive control, respectively. Three hours later, the erythrocyte suspensions were centrifuged and the color of the supernatants was compared with controls. If the supernatant solution was absolute achromatic, it was implied that PTX-NPs did not induce any hemolysis. In contrast, the PTX-NPs would induce hemolysis if the supernatant solution was red.

*2.2.7. Maximum tolerated dose (MTD)*

MTD studies for PTX-NPs and clinically used formulation (TAXOL®) were carried out in healthy Balb/c female mice. In the single dose study, healthy female mice were conducted with 6 animals per group. Ten groups of mice received i.v. injection of 15, 25, 35, 45 mg PTX/kg b.w of TAXOL® and 30, 40, 60, 80, 100 mg PTX/kg b.w of PTX-NPs and normal saline as a control through tail vein. The volume given i.v. was 0.2–0.3 ml. The MTD was defined as the allowanced of a median body weight loss of approximately 15% of the control and cause neither death due to toxic effects nor remarkable changes in the general signs within one week after administration (Discher and Eisenberg, 2002).

*2.2.8. Pharmacokinetic and tissue distribution studies*

Healthy SD mice (6 weeks, 200 ± 20 g) were injected through the tail vein with 4 mg/kg (consulted with the clinical dose for human) of Taxol® and PTX-NPs. Then withdrew blood from the rat tail vein at 0.083, 0.5, 1, 2, 4, 6, 8, 10, 12, 24 h, and samples were centrifuged at the rate of 10,000 r/min and harvested 100 μl of upper plasma to determine. The blood concentration–time curve was calculated. The determined approach was as follows: 100 μl samples of plasma were mixed with 20 μl of levonorgestrel solution in methanol (29.4 μg/ml) as the internal standard and then added 300 μl of ethyl acetate–hexane (1:1 v/v). The samples were vortexed at the rate of 2500 r/min for 5 min, and then centrifuged at the rate of 12,000 r/min for 10 min. After that the organic layer was transferred to a clean tube and evaporated to dryness under blowing nitrogen gas at 40 °C. The extraction residue was reconstituted in 50 μl of methanol and centrifuged at the rate of 16,000 r/min for 5 min, and 20 μl of upper solution was injected into the HPLC system. The determined approach of HPLC was the same as the method of LE.

*2.2.8.1. Tissue distribution studies.* 4T1 breast cancer cells ($2 \times 10^5$ cells) were inoculated into female SPF Balb/c mice (8 weeks, 20 ± 2 g), when tumors were approximately 80–200 $mm^3$ in size, the mice were randomly divided into three groups ($n = 75$), Two groups were given a single i.v. injection of 4 mg PTX/kg b.w of Taxol® and PTX-NPs. The third group was injected with 10 mg PTX/kg b.w of PTX-NPs. Five mice were sacrificed at 0.5, 2, 6, 12 and 24 h after drug administration. Samples of plasma, liver, kidney, spleen, lung, heart, brain and tumor were harvested and stored at −20 °C until detected. The concentrations of PTX in various tissues at different time were calculated. The determined approach was as follows: tissue samples were homogenized (ultra-turraxT10 basic, IKA, Germany) in 0.25 ml normal saline first, then extracted and determined as described above.

## 3. Results

### 3.1. Selection of MPEG–PCL copolymer and nanoparticles preparative methods

Table 1 shows the result of preparation of PTX-NPs with different *Mn* ratios of MPEG–PCL copolymer and different preparative methods. The result shown that $MPEG_{2000}$–$PCL_{2000}$ was very suitable to prepare PTX-NPs, and the PDI was only 0.10, which also proved the NPs had an uniform particle size distribution. This experiment verified the theory that the fraction ($f$) of the hydrophilic domain relative to molecular weight is controlled within a certain range ($f > 0.42$) generally form spherical micelles (Discher and Eisenberg, 2002).

Dialysis method is one of the most extensively used methods. However, as the results of experiment as shown in Table 2, DL, EE and Y were not ideal. Last but most important, most of particle sizes were more than 100 nm (Fig. 1), and these sizes cannot meet the requirements of EPR effect. Compared with dialysis method, freeze-drying is a simple, valuable tool to prepare nanoparticles. EE was almost 100%. The mean size was 33.1 ± 0.5 nm, PDI was 0.17. However, this procedure worked with poisonous organic solvent TBA. This was limited in practical applications.

By solid dispersion technique, PTX could be successfully incorporated into MPEG–PCL copolymer. The prepared NPs had the highest DL (25.6%), EE (99.5%) and uniform size distribution

**Table 1**
PTX-NPs prepared from MPEG–PCL copolymers with different molecular weight ratios.

| MPEGx–PCLy | Drug loading (%)[a] | Encapsulation efficiency (%)[a] | Particle size (nm) | Polydispersity index | Stability (25 °C) |
|---|---|---|---|---|---|
| $MPEG_{750}$–$PCL_{2000}$ | – | – | – | – | – |
| $MPEG_{2000}$–$PCL_{2000}$ | 8.1 ± 0.1 | 99.3 ± 0.2 | 28.6 ± 1.1 | 0.10 ± 0.1 | 7 h |
| $MPEG_{2000}$–$PCL_{4000}$ | 8.3 ± 0.1 | 99.7 ± 0.3 | 153.5 ± 2.2 | 0.99 ± 0.1 | 4 h |
| $MPEG_{2000}$–$PCL_{8000}$ | – | – | – | – | – |
| $MPEG_{5000}$–$PCL_{2000}$ | 8.1 ± 0.2 | 99.8 ± 0.3 | 406.1 ± 5.6 | 0.47 ± 0.2 | 5 h |

X: MPEG Theoretical molecular weight.
Y: PCL Theoretical molecular weight.
[a] The amount of PTX in the solution was determined by HPLC.
"–" PTX-NPs cannot be prepared or was extremely instable.
Data represent mean ± SD ($n$ = 3).

**Table 2**
Nanoparticles preparation with different methods.

| Method | Drug loading (%)[a] | Encapsulation efficiency (%)[a] | Yield (%) | Particle size (nm) | Polydispersity index |
|---|---|---|---|---|---|
| Dialysis method | 0.4 ± 0.9 | 5.4 ± 0.5 | 3.1 ± 1.2 | 42.3 ± 2.5 | 0.77 ± 0.1 |
| Solid dispersion technique | 8.1 ± 0.3 | 99.3 ± 0.6 | 99.8 ± 0.5 | 28.6 ± 0.1 | 0.10 ± 0.2 |
| Freeze-drying | 8.3 ± 0.2 | 99.9 ± 1.1 | 99.97 ± 1.1 | 33.1 ± 0.5 | 0.17 ± 0.1 |

[a] The amount of PTX in the solution was determined by HPLC.
Data represent mean ± SD ($n$ = 3).

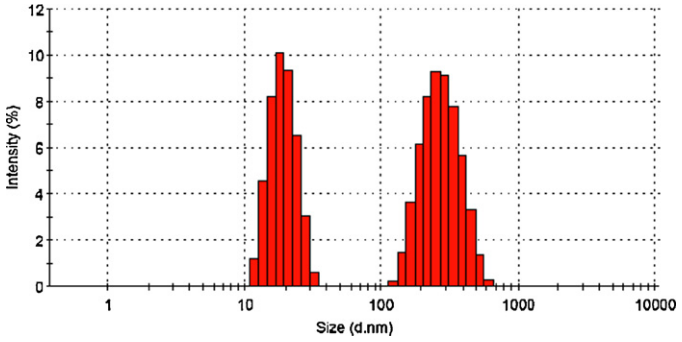


**Fig. 1.** The size distribution of PTX-NPs prepared by dialysis method.

(PDI = 0.10) as shown in Table 2. Remarkable features of our preparation procedure (Fig. 2) included the formation of a clear polymer/drug solution without toxic organic solvent, moreover, the alcohol could be recycled which can greatly reduce the cost of production. Furthermore, the freeze-drying powder without cryoprotector could be stored at room temperature for more than six months and easy to be rehydrated with water. Unlike other drug incorporation methods, which contained toxic organic solvent or dialysis steps or time-consuming emulsification, our preparation period was too short to increase any related substances of PTX. Last but not least, the polymeric material had good biodegradability and

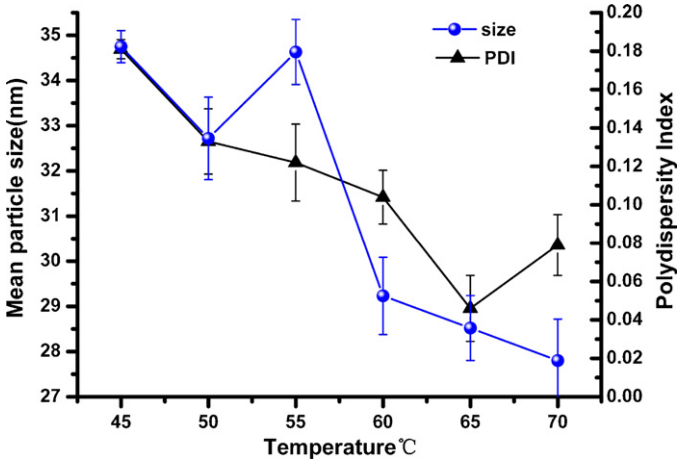


**Fig. 3.** Effect of temperature on PDI and particle size of PTX-NPs (DL = 8%). Each point represents mean ± SD. Error bars represent the standard deviation ($n$ = 3).

the preparation technology was easy to realize sterile manufacturing in compliance with good manufacturing practice.

Besides the factors of drug loading and the length of the hydrophobic segment, we found the temperature had great influences on the particle size and PDI. Therefore, we studied the mean

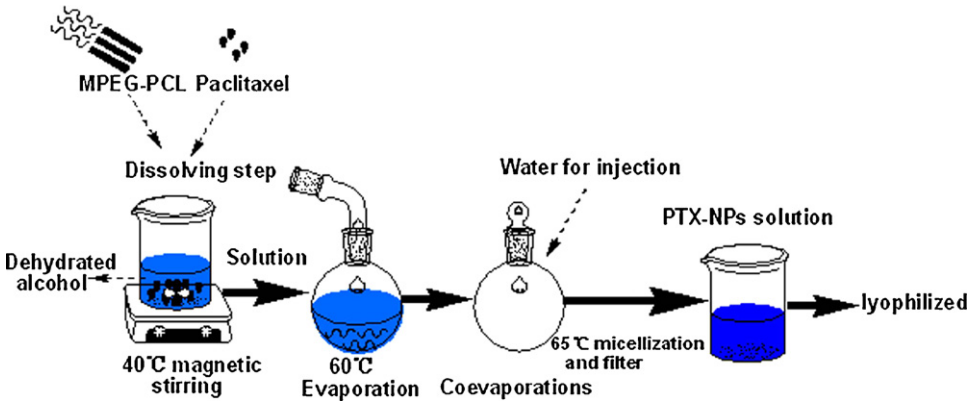


**Fig. 2.** Scheme of the solid dispersion technique preparative procedure.


**Fig. 4.** Morphology of PTX-NPs. (A) Water, (B) Blank MPEG–PCL NPs (33 mg/ml), (C) PTX-NPs (DL = 8%), (D) PTX-NPs freeze-dried powder, (E) Re-dispersed freeze-dried PTX-NPs with water (DL = 8%).

size and distribution of the nanoparticles under different preparation temperatures which were 45, 50, 55, 60, 65, 70, 75, 80 °C, respectively, as shown in Fig. 3. The smallest mean particle size of NPs was 27.2 nm and PDI was 0.07 at 75 °C. However, the temperature is not good for chemical stability of PTX, so that the temperature 65 °C was an optimal preparation temperature.

### 3.2. Characterization of PTX-NPs

PTX-NPs were prepared by solid dispersion technique using MPEG–PCL copolymer. The highest DL was 25.6%, the particle size

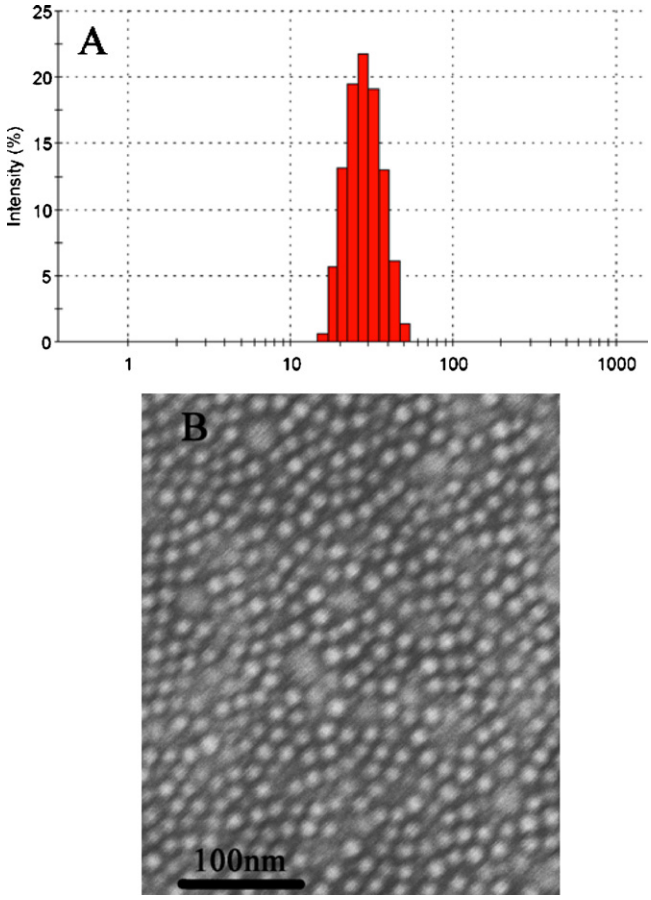


**Fig. 5.** PTX-NPs prepared by solid dispersion technique: (A) Particles size, (B) TEM image. Scale bars were 150 nm.

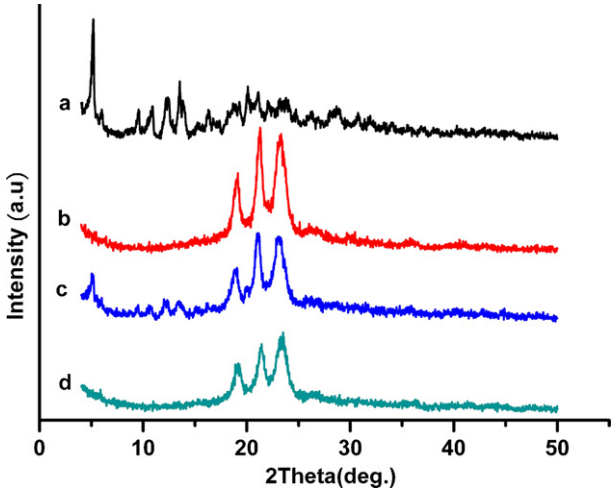


**Fig. 6.** Powder X-ray diffraction patterns for PTX and MPEG–PCL materials. (a) PTX, (b) Blank $MPEG_{2000}$–$PCL_{2000}$ polymer, (c) physical mixtures of PTX and $MPEG_{2000}$–$PCL_{2000}$ (8:92), (d) PTX-NPs (DL = 8%).

ranged from 27.6 nm to 53.1 nm when the initial amount of PTX was <28% (DL), and the particle size would increase gradually with increasing amount of loaded PTX. In our experiments, the reconstituted solution (DL = 8.0%) was stable for 7 h at room temperature (Table 3), and 7 h of stable time was sufficient to meet the requirement of clinical infusion. Besides, the solution can be stable for 5 days at 4 °C, stable time became shorter with the increase of DL. The reasons maybe that MPEG–PCL copolymer dissolved in solution was not enough to entrap and stabilize more PTX or hydration layer which formed by MPEG was too thin to sustain its micellar structure.

The appearance of PTX-NPs was shown in Fig. 4, and the clear solution could be observed. The PTX-NPs (DL = 8%) was chosen to characterize in detail. The mean size of PTX-NPs was about 27.6 nm (Fig. 5A). Fig. 5B shows TEM image of PTX-NPs. The TEM image clearly revealed that PTX-NPs were uniform and spherical shapes in solution, and the sizes consisted with the result characterized by Malvern Nano-ZS 90 laser particle size analyzer.

Crystallographic assay was performed by XRD and the result was presented in Fig. 6. In comparison with XRD diagram of PTX, blank MPEG–PCL copolymer, and physical mixtures of PTX and MPEG–PCL copolymer (8:92), the absence of specific diffraction peaks in diagram of PTX-NPs (DL = 8%) indicated that PTX was completely encapsulated within their core-shell structure amorphously.

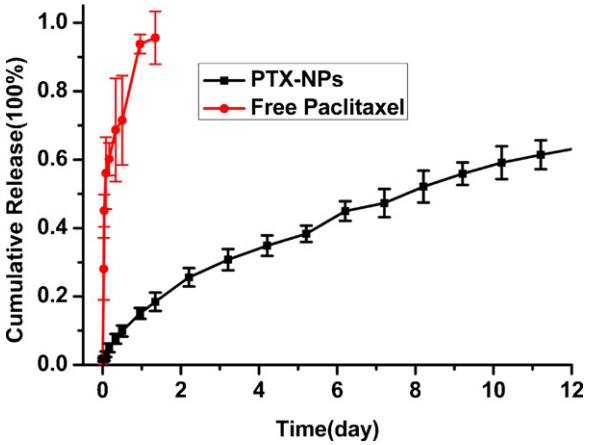


**Fig. 7.** *In vitro* release curve of PTX-NPs and free PTX solution. Each point represents mean ± SD for three samples. Error bars represent the standard deviation ($n = 3$).

**Table 3**
Drug-loading and encapsulation efficiency of PTX-NPs.

| Sample no. | Drug feeding (wt%) | Drug loading (%)[a] | Encapsulation efficiency (%)[a] | Particle size (nm) | Polydispersity index | Stability | |
|---|---|---|---|---|---|---|---|
| | | | | | | 4 °C | 25 °C |
| 1 | 5.8 | 5.7 ± 0.8 | 98.3 ± 1.1 | 27.6 ± 0.2 | 0.05 ± 0.02 | 7 d | 9 h |
| 2 | 8.2 | 8.1 ± 1.1 | 98.8 ± 1.3 | 28.6 ± 0.1 | 0.11 ± 0.03 | 5 d | 7 h |
| 3 | 11.2 | 11.0 ± 1.2 | 98.2 ± 0.9 | 41.9 ± 2.9 | 0.39 ± 0.01 | 4 d | 4 h |
| 4 | 15.0 | 14.8 ± 0.9 | 98.7 ± 0.7 | 44.1 ± 1.1 | 0.21 ± 0.03 | 2 d | 3 h |
| 5 | 20.2 | 20.1 ± 1.3 | 99.5 ± 1.1 | 53.1 ± 2.2 | 0.43 ± 0.02 | 10 h | 0.5 h |
| 6 | 28.0 | 25.6 ± 1.5 | 91.4 ± 2.1 | – | – | 1 h | 0.15 h |

[a] The amount of PTX in the solution was determined by HPLC.
"–" PTX-NPs can be prepared, however, the freeze-drying powder cannot be reconstituted.
Data represent mean ± SD ($n$ = 3).

### 3.3. *In vitro* drug release behavior

Fig. 7 showed the *in vitro* release profiles of PTX from PTX-NPs and free PTX. Free PTX exhibited a rapid release behavior and more than 95% of drug was released within 32 h, thus it demonstrated that the dialysis membrane had no effect on retarding the release of the drug from nanoparticles. In contrast, the experiments showed only about 30% of initial loading amount released from the PTX-NPs in 12 days. We studied the release kinetics equations of PTX-NPs, and the results were shown in Table 4. The results of fitting models of PTX-NPs *in vitro* release showed it had the best fit for the Higuchi model, because its coefficient is the largest. So it demonstrated *in vitro* drug release behavior was dominated by diffusion mechanism. However, the characteristic parameters of drug release mechanism of $n$ in Korsmeyer–Peppas was equal to 0.6186, between 0.45 and 0.89, this showed that PTX released from the NPs was actually a result of a combination of drug diffusion and polymer materials corrosion degradation. Moreover diffusion-controlled release behavior dominated in the release process.

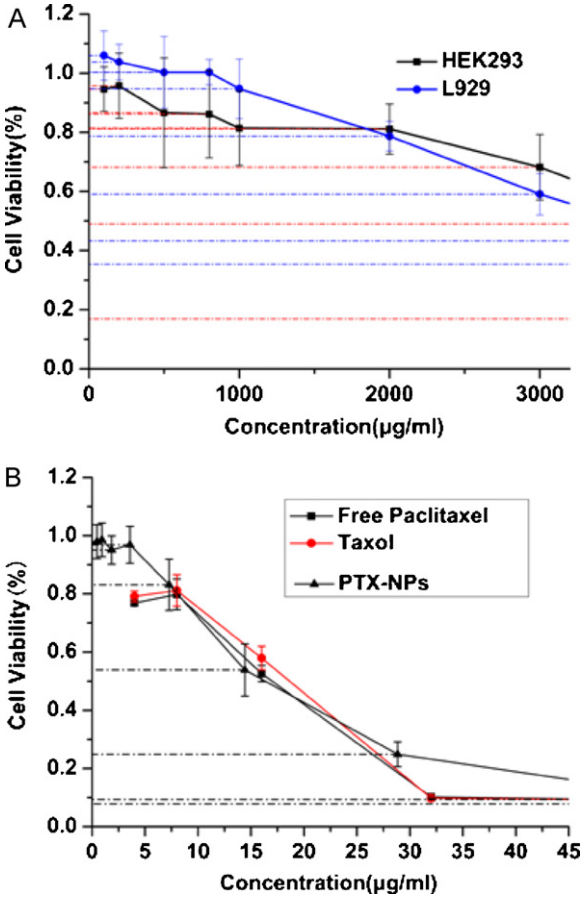


**Fig. 8.** (A) Cytotoxicity of blank MPEG–PCL polymer at different concentrations on HEK293 cells and L929 cells. (B) Cytotoxicity of free PTX, Taxol® and PTX-NPs at different concentrations of PTX on murine breast cancer cell 4T1. Error bars represent the standard deviation ($n$ = 6).

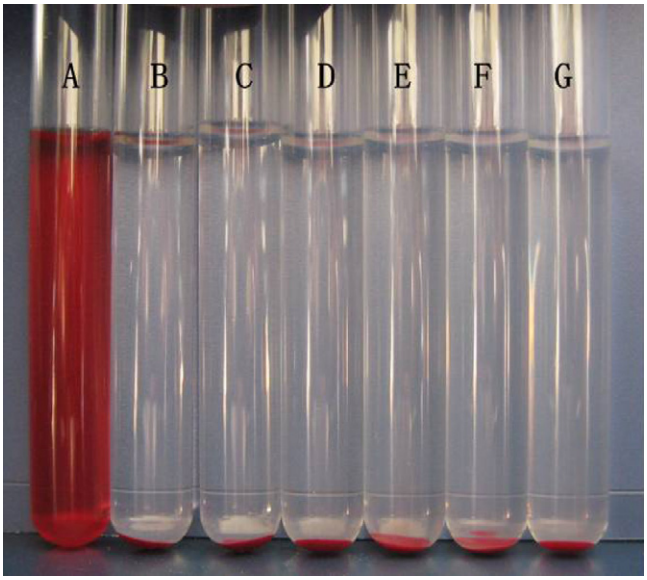


**Fig. 9.** Hemolytic test: (A) distilled water as positive control; (B) normal saline as negative control; (C) 50 mg/ml of blank NPs in saline solution; (D) 0.4 mg/ml of PTX of PTX-NPs in saline solution; (E) 0.8 mg/ml of PTX of PTX-NPs in saline solution; (F) 1.0 mg/ml of PTX of PTX-NPs in saline solution; (G) 1.6 mg/ml of PTX of PTX-NPs in saline solution.

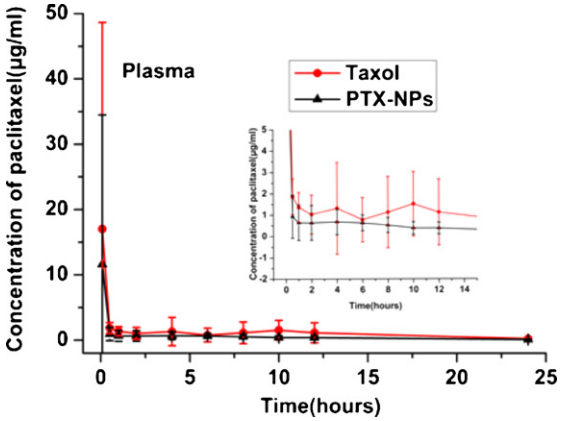


**Fig. 10.** The blood concentration–time curve in mice plasma after i.v. administration of equal dose of 4 mg PTX/kg b.w of Taxol® and PTX-NPs. Error bars represent the standard deviation ($n$ = 6).

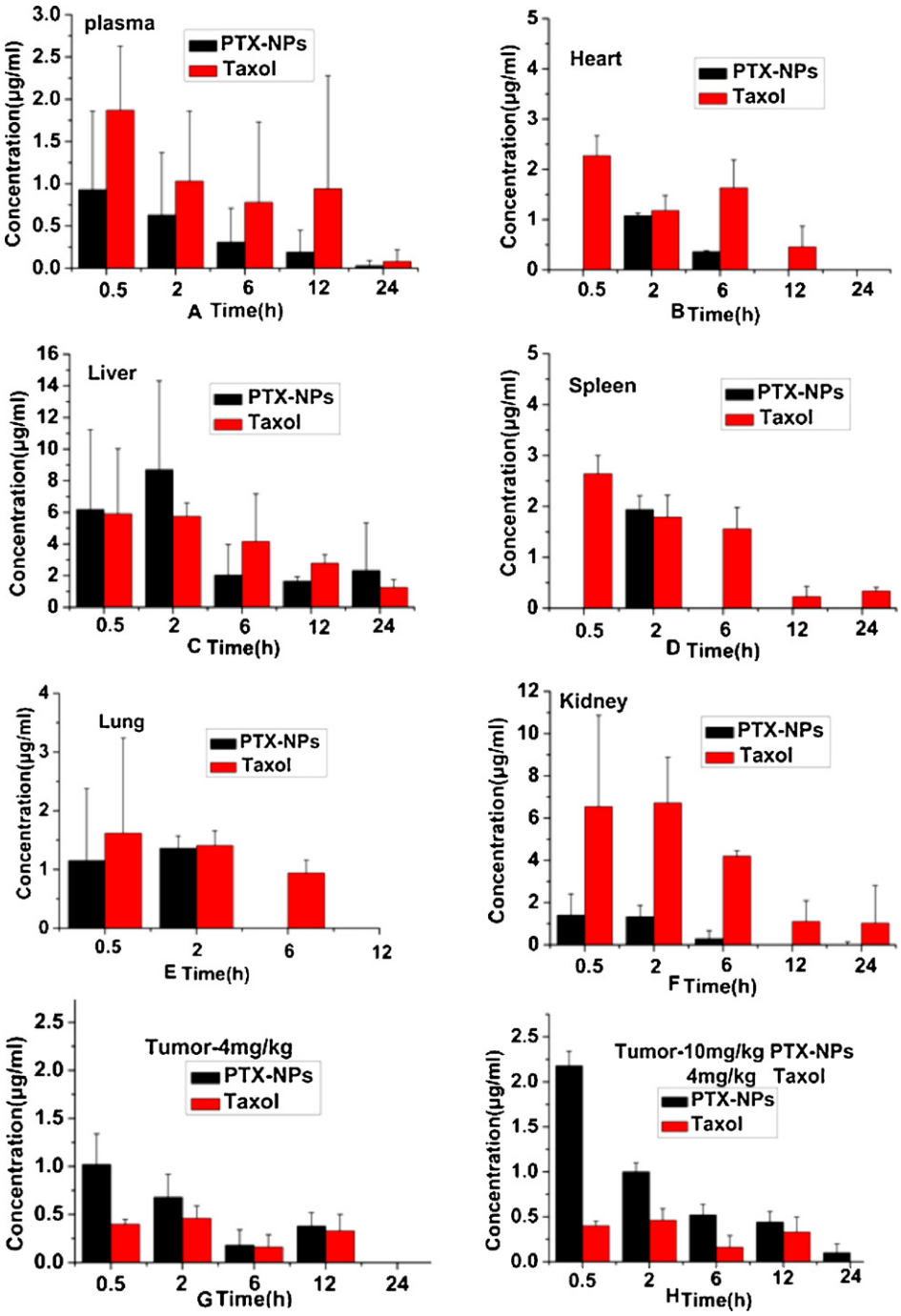


**Fig. 11.** Tissue distribution of PTX determined in Balb/c mice after i.v. administration of Taxol® and PTX-NPs at different time. After i.v. administration 4 mg PTX/kg b.w of Taxol® and PTX-NPs, the concentration of PTX at different time in mice plasma (A), heart (B), liver (C), spleen (D), lung (E), kidney (F), tumor(G), respectively. After i.v. administration 4 mg PTX/kg b.w of Taxol® and 10 mg PTX/kg b.w of PTX-NPs, the concentration of PTX at different time in mice tumor (H). Error bars represent the standard deviation ($n = 5$).

**Table 4**
The release kinetics equations of PTX-NPs.

| Model | Equations | $r$ |
|---|---|---|
| Zero order: $M_t = nt + K$ | $M_t = 0.0976t + 3.5953$ | 0.9788 |
| First order: $\ln(100 - M_t) = nt + K$ | $\ln(100 - M_t) = -0.0012t + 4.5708$ | 0.9864 |
| Higuchi: $M_t = nt^{1/2} - K$ | $M_t = 1.7685t^{1/2} - 1.3531$ | 0.9991 |
| Korsmeyer–Peppas: $\ln M_t = n \ln t - K$ | $\ln M_t = 0.6186 \ln t - 0.0869$ | 0.9990 |

$t$: time; $M_t$: the cumulative release of the drug at $t$ time; $k$: the kinetic constant; $n$: the release exponent; $r$: correlation coefficients.

### 3.4. Cell viability assay

Blank MPEG–PCL polymeric material was evaluated for its cytotoxicity against HEK 293 and L929 cells with an MTT assay. As shown in Fig. 8A, the concentration causing 50% of cell killing was about 3 mg/ml calculated by curve fitting using SPSS software. *In vitro* anticancer activity of PTX-NPs was performed by using murine breast cancer cell 4T1 compared with free PTX and Taxol®. Fig. 8B shows all three formulations of PTX had similar $IC_{50}$, which were approximate 18 μg/ml. The results demonstrated the PTX-NPs had equivalent cytotoxic activity *in vitro* with free PTX and Taxol®.

### 3.5. In vitro hemolytic test

*In vitro* hemolytic tests of PTX-NPs were performed using 2% rabbit erythrocyte suspension. As shown in Fig. 9, the blank MPEG–PCL copolymer (50 mg/ml) and the PTX-NPs (0.4 mg/ml, 0.8 mg/ml, 1 mg/ml, 1.6 mg/ml of PTX) in saline solution did not cause any hemolysis on rabbit erythrocyte comparing with the negative control (normal saline).

### 3.6. Maximum tolerated dose

The studies showed that with a single dose intravenous administration of 35 mg PTX/kg b.w of Taxol®, the mice showed an extremely painful condition, and administration of 40 mg PTX/kg b.w of Taxol®, the mice directly died. Therefore the MTD of Taxol® administered was approximate 30 mg PTX/kg b.w by the i.v. route. However, we were unable to find the MTD of PTX-NPs formulations administered in a single dose because of the largest concentration of PTX in the formulations was 8 mg/ml and the limitation of injection volume was 0.3 ml. When 80 mg PTX/kg b.w was administrated intravenously, the mice showed no painful condition. So we studied multiple doses of 60 mg PTX/kg b.w twice in 1 h, the result showed that the mice were in painful condition but still alive after the administration of 120 mg PTX/kg b.w of PTX-NPs. Therefore, the MTD of PTX-NPs formulations was >80 mg PTX/kg b.w (single dose) and <120 mg PTX/kg b.w.

### 3.7. Pharmacokinetic and tissue distribution studies

After administration of 4 mg PTX/kg b.w of Taxol® and PTX-NPs, the peak of plasma concentration ($C_{max}$) obtained was $4.80 \pm 2.59$ μg/ml and $1.60 \pm 2.79$ μg/ml, respectively. The time of maximum concentration ($T_{max}$) and the area under the plasma concentration–time curve ($AUC_{0-\infty}$) were $0.74 \pm 1.60$ h, $22.00 \pm 6.40$ μg h/ml and $0.08 \pm 0.02$ h, $8.43 \pm 2.38$ μg h/ml for Taxol® and PTX-NPs, respectively. The blood concentration–time curve was shown in Fig. 10. From the results of experiment, the blood concentration of PTX-NPs in plasma was lower than Taxol® at the same time. The cause may be that PTX-NPs were distributed to various tissues from blood vessels rapidly.

The concentration of PTX in various tissues at different time was calculated, the results were presented in Fig. 11. After i.v. administration, PTX was soon distributed into various tissues in 0.5 h. The results shown the tissue distribution of PTX after i.v., administration of PTX-NPs was obviously different from that of Taxol®. The concentration of PTX administrated PTX-NPs was lower than that of Taxol® at all time points in each normal tissues except liver. However, the concentration of PTX administrated PTX-NPs was higher than that of Taxol® in the tumor. Above all, administration of 10 mg PTX/kg b.w of PTX-NPs, the levels of PTX in the tumors increased proportionally. These results signified PTX-NPs could reduce the damage of PTX on normal tissue and side effects. Furthermore, it could improve antitumor efficacy through increasing the dose of PTX-NPs.

## 4. Discussion

Chemotherapy, as a conventional treatment of cancer, was widely used in clinical while the side-effects were very severe. Thus, many scientists were trying to find new drug delivery systems (DDS) which could reduce systemic circulation of the drug leading to higher therapeutic efficacy and lower systemic toxicity. Now we prepared PTX-NPs using biodegradable amphiphilic diblock copolymer MPEG–PCL through solid dispersion technique without organic solvent. Moreover, the DL and LE were higher than PTX formulations reported previously (Kim and Lee, 2001; Letchford et al., 2009), and the particle size and uniform size distribution were extremely good without any special adjustment. Meanwhile the results disproved the previous prediction which PTX was not highly compatible with PCL than PDLLA (Letchford et al., 2009). In experiment, we could not achieve PTX loading levels of 20% using the dialysis method (Kim and Lee, 2001). Moreover, the Y% of dialysis method was very low. It may be the differences of hydrophobic block length which were responsible for the variable PTX loadings. Furthermore, the results of pharmacokinectics and tissue distribution studies revealed the nanoscale preparations of paclitaxel had advantages over reducing toxicities and improving therapeutic effect to treat solid tumors. It provided the potential application in clinical research.

## 5. Conclusions

In this paper, we have successfully prepared an injectable, biocompatible, biodegradable, targeted, safe, effective and controlled release nanoscale preparation, which may be significant to promote more nanoscale preparations for hydrophobic drug to be applied into clinical practice.

## Acknowledgements

This work was financially supported by National 863 project (2007AA021902 and 2007AA021804), National Natural Science Foundation of China (NSFC20704027), Sichuan Key Project of Science and Technology (2007SGY019), Sichuan Prominent Young Talents Program (07ZQ026-033), and Chinese Key Basic Research Program (2004CB518807).

## References

Beletsi, A., Klepetsanis, P., Ithakissios, D.S., Kounias, S., Stavropoulos, A., Avgoustakis, K., 2008. Simultaneous optimization of cisplatin-loaded PLGA-mPEG nanoparticles with regard to their size and drug encapsulation. Curr. Nanosci. 4, 173–178.
Cha, E.-J., Kim, J.E., Ahn, C.-H., 2009. Stabilized polymeric micelles by electrostatic interactions for drug delivery system. Eur. J. Pharm. Sci. 38, 341–346.
Chan, J.M., Zhang, L., Yuet, K.P., Liao, G., Rhee, J.-W., Langer, R., Farokhzad, O.C., 2009. PLGA-lecithin-PEG core-shell nanoparticles for controlled drug delivery. Biomaterials 30, 1627–1634.
Chang, Y.-C., Chu, I.M., 2008. Methoxy poly(ethylene glycol)-b-poly(valerolactone) diblock polymeric micelles for enhanced encapsulation and protection of camptothecin. Eur. Polym. J. 44, 3922–3930.
Chavanpatil, M.D., Patil, Y., Panyam, J., 2006. Susceptibility of nanoparticle-encapsulated paclitaxel to P-glycoprotein-mediated drug efflux. Int. J. Pharm. 320, 150–156.
Chu, H., Liu, N., Wang, X., Jiao, Z., Chen, Z., 2009. Morphology and in vitro release kinetics of drug-loaded micelles based on well-defined PMPC-b-PBMA copolymer. Int. J. Pharm. 371, 190–196.
Discher, D.E., Eisenberg, A., 2002. Polymer vesicles. Science 297, 967–973.
Dong, P., Wang, X., Gu, Y., Wang, Y., Wang, Y., Gong, C., Luo, F., Guo, G., Zhao, X., Wei, Y., Qian, Z., 2010. Self-assembled biodegradable micelles based on star-shaped PCL-b-PEG copolymers for chemotherapeutic drug delivery. Colloids Surf. A: Physicochem. Eng. Aspects 358, 128–134.
Dong, Y., Feng, S.-S., 2004. Methoxy poly(ethylene glycol)-poly(lactide) (MPEG-PLA) nanoparticles for controlled delivery of anticancer drugs. Biomaterials 25, 2843–2849.
Dong, Y., Feng, S.-S., 2007. In vitro and in vivo evaluation of methoxy polyethylene glycol-polylactide (MPEG-PLA) nanoparticles for small-molecule drug chemotherapy. Biomaterials 28, 4154–4160.
Duan, Y.R., Sun, X., Gong, T., Wang, Q., Zhang, Z.R., 2006. Preparation of DHAQ-loaded mPEG-PLGA-mPEG nanoparticles and evaluation of drug release behaviors in vitro/in vivo. J. Mater. Sci. Mater. Med. 17, 509–516.
Fournier, E., Dufresne, M.H., Smith, D.C., Ranger, M., Leroux, J.C., 2004. A novel one-step drug loading procedure for water-soluble amphiphilic nanocarriers (vol. 21, p. 962, 2004). Pharm. Res. 23, 1948–11948.
Gao, J., Ming, J., He, B., Fan, Y., Gu, Z., Zhang, X., 2008. Preparation and characterization of novel polymeric micelles for 9-nitro-20(S)-camptothecin delivery. Eur. J. Pharm. Sci. 34, 85–93.
Gaucher, G., Marchessault, R.H., Leroux, J.-C., 2010. Polyester-based micelles and nanoparticles for the parenteral delivery of taxanes. J. Control. Release 143.
Gong, J., Huo, M., Zhou, J., Zhang, Y., Peng, X., Yu, D., Zhang, H., Li, J., 2009. Synthesis, characterization, drug-loading capacity and safety of novel octyl modified serum albumin micelles. Int. J. Pharm. 376, 161–168.

Gryparis, E.C., Mattheolabakis, G., Bikiaris, D., Avgoustakis, K., 2007. Effect of conditions of preparation on the size and encapsulation properties of PLGA-mPEG nanoparticles of cisplatin. Drug Deliv. 15, 371–380.
Hammady, T., Rabanel, J.-M., Dhanikula, R.S., Leclair, G., Hildgen, P., 2009. Functionalized nanospheres loaded with anti-angiogenic drugs: cellular uptake and angiosuppressive efficacy. Eur. J. Pharm. Biopharm. 72, 418–427.
He, G., Ma, L.L., Pan, J., Venkatraman, S., 2007. ABA and BAB type triblock copolymers of PEG and PLA: a comparative study of drug release properties and "stealth" particle characteristics. Int. J. Pharm. 334, 48–55.
Jackson, J.K., Smith, J., Letchford, K., Babiuk, K.A., Machan, L., Signore, P., Hunter, W.L., Wang, K., Burt, H.M., 2004. Characterization of perivascular poly(lactic-co-glycolic acid) films containing paclitaxel. Int. J. Pharm. 283, 97–109.
Jaromin, A., Zarnowski, R., Kozubek, A., 2006. Emulsions of oil from *Adenanthera pavonina* L. seeds and their protective effect. Cell. Mol. Biol. Lett. 11, 438–448.
Jette, K.K., Law, D., Schmitt, E.A., Kwon, G.S., 2004. Preparation and drug loading of poly(ethylene glycol)-block-poly(epsilon-caprolactone) micelles through the evaporation of a cosolvent azeotrope. Pharm. Res. 21, 1184–1191.
Jin, C., Bai, L., Wu, H., Tian, F., Guo, G., 2007. Radiosensitization of paclitaxel, etanidazole and paclitaxel + etanidazole nanoparticles on hypoxic human tumor cells in vitro. Biomaterials 28, 3724–3730.
Katsikogianni, G., Avgoustakis, K., 2006. Poly(lactide-co-glycolide)-methoxy-poly(ethy lene glycol) nanoparticles: drug loading and release properties. J. Nanosci. Nanotechnol. 6, 3080–3086.
Kim, S.C., Kim, D.W., Shim, Y.H., Bang, J.S., Oh, H.S., Kim, S.W., Seo, M.H., 2001. *In vivo* evaluation of polymeric micellar paclitaxel formulation: toxicity and efficacy. J. Control. Release 72, 191–202.
Kim, S.Y., Lee, Y.M., 2001. Taxol-loaded block copolymer nanospheres composed of methoxy poly(ethylene glycol) and poly([var epsilon]-caprolactone) as novel anticancer drug carriers. Biomaterials 22, 1697–1704.
Ko, J., Park, K., Kim, Y.-S., Kim, M.S., Han, J.K., Kim, K., Park, R.-W., Kim, I.-S., Song, H.K., Lee, D.S., Kwon, I.C., 2007. Tumoral acidic extracellular pH targeting of pH-responsive MPEG-poly([beta]-amino ester) block copolymer micelles for cancer therapy. J. Control. Release 123, 109–115.
Lee, S.Y., Hyun, H., Youn, J.Y., Kim, B.S., Song, I.B., Kim, M.S., Lee, B., Khang, G., Lee, H.B., 2008. Preparation of nano-emulsified paclitaxel using MPEG-PLGA diblock copolymers. Colloids Surf. A: Physicochem. Eng. Aspects 313–314, 126–130.
Letchford, K., Liggins, R., Wasan, K.M., Burt, H., 2009. *In vitro* human plasma distribution of nanoparticulate paclitaxel is dependent on the physicochemical properties of poly(ethylene glycol)-block-poly(caprolactone) nanoparticles. Eur. J. Pharm. Biopharm. 71, 196–206.
Li, F., Li, J., Wen, X., Zhou, S., Tong, X., Su, P., Li, H., Shi, D., 2009. Anti-tumor activity of paclitaxel-loaded chitosan nanoparticles: an in vitro study. Mater. Sci. Eng. C 29, 2392–2397.
Li, J., Zhai, Y.L., Zhang, B., Deng, L.D., Xu, Y.S., Dong, A.J., 2008. Methoxy poly(ethylene glycol)-block-poly(D,L-lactic acid) copolymer nanoparticles as carriers for transdermal drug delivery. Polym. Int. 57, 268–274.
Liu, Y., Chen, G.S., Li, L., Zhang, H.Y., Cao, D.X., Yuan, Y.J., 2003. Inclusion complexation and solubilization of paclitaxel by bridged bis(beta-cyclodextrin)s containing a tetraethylenepentaamino spacer. J. Med. Chem. 46, 4634–4637.
Maeda, H., Wu, J., Sawa, T., Matsumura, Y., Hori, K., 2000. Tumor vascular permeability and the EPR effect in macromolecular therapeutics: a review. J. Control. Release 65, 271–284.
Matsumura, Y., 2008. Poly (amino acid) micelle nanocarriers in preclinical and clinical studies. Adv. Drug Deliv. Rev. 60, 899–914.
Miglietta, A., Cavalli, R., Bocca, C., Gabriel, L., Rosa Gasco, M., 2000. Cellular uptake and cytotoxicity of solid lipid nanospheres (SLN) incorporating doxorubicin or paclitaxel. Int. J. Pharm. 210, 61–67.
Misra, R., Acharya, S., Dilnawaz, F., Sahoo, S.K., 2009. Sustained antibacterial activity of doxycycline-loaded poly(D,L-lactide-co-glycolide) and poly(epsilon-caprolactone) nanoparticles. Nanomedicine 4, 519–530.
Mo, Y., Lim, L.-Y., 2005. Paclitaxel-loaded PLGA nanoparticles: potentiation of anticancer activity by surface conjugation with wheat germ agglutinin. J. Control. Release 108, 244–262.
Mu, C.-F., Balakrishnan, P., Cui, F.-D., Yin, Y.-M., Lee, Y.-B., Choi, H.-G., Yong, C.S., Chung, S.-J., Shim, C.-K., Kim, D.-D., 2010. The effects of mixed MPEG-PLA/Pluronic copolymer micelles on the bioavailability and multidrug resistance of docetaxel. Biomaterials 31, 2371–2379.
Musumeci, T., Ventura, C.A., Giannone, I., Ruozi, B., Montenegro, L., Pignatello, R., Puglisi, G., 2006. PLA/PLGA nanoparticles for sustained release of docetaxel. Int. J. Pharm. 325, 172–179.
Ngawhirunpat, T., Wonglertnirant, N., Opanasopit, P., Ruktanonchai, U., Yoksan, R., Wasanasuk, K., Chirachanchai, S., 2009. Incorporation methods for cholic acid chitosan-g-mPEG self-assembly micellar system containing camptothecin. Colloids Surf. B Biointerfaces 74, 253–259.
Önyüksel, H., Jeon, E., Rubinstein, I., 2009. Nanomicellar paclitaxel increases cytotoxicity of multidrug resistant breast cancer cells. Cancer Lett. 274, 327–330.
Ravi Kumar, M.N.V., Bakowsky, U., Lehr, C.M., 2004. Preparation and characterization of cationic PLGA nanospheres as DNA carriers. Biomaterials 25, 1771–1777.
Rowinsky, E.K., Eisenhauer, E.A., Chaudhry, V., 1993. Clinical toxicities encountered with paclitaxel (Taxol). Semin. Oncol. 3, 1–15.
Sheikh, F.A., Barakat, N.A.M., Kim, B.-S., Aryal, S., Khil, M.-S., Kim, H.-Y., 2009. Self-assembled amphiphilic polyhedral oligosilsesquioxane (POSS) grafted poly(vinyl alcohol) (PVA) nanoparticles. Mater. Sci. Eng. C 29, 869–876.
Terwogt, J.M.M., Nuijen, B., Huinink, W.W.T., Beijnen, J.H., 1997. Alternative formulations of paclitaxel. Cancer Treat. Rev. 23, 87–95.
van Hasselt, P.M., Janssens, G.E.P.J., Slot, T.K., van der Ham, M., Minderhoud, T.C., Talelli, M., Akkermans, L.M., Rijcken, C.J.F., van Nostrum, C.F., 2009. The influence of bile acids on the oral bioavailability of vitamin K encapsulated in polymeric micelles. J. Control. Release 133, 161–168.
Vyas, D.M., Vittorio, F., 1995. 3 Paclitaxel (taxol) Formulation and Prodrugs, Pharmacochemistry Library. Elsevier, pp. 103–130.
Wall, M.E., 1998. Camptothecin and taxol: discovery to clinic. Med. Res. Rev. 18, 299–314.
Wang, Y., Yu, L., Han, L., Sha, X., Fang, X., 2007. Difunctional pluronic copolymer micelles for paclitaxel delivery: synergistic effect of folate-mediated targeting and pluronic-mediated overcoming multidrug resistance in tumor cell lines. Int. J. Pharm. 337, 63–73.
Wei, X., Gong, C., Gou, M., Fu, S., Guo, Q., Shi, S., Luo, F., Guo, G., Qiu, L., Qian, Z., 2009. Biodegradable poly([var epsilon]-caprolactone)-poly(ethylene glycol) copolymers as drug delivery system. Int. J. Pharm. 381, 1–18.
Weiss, R.B., Donehower, R.C., Wiernik, P.H., 1990. Hypersensitivity reactions from taxol. J. Clin. Oncol. 8, 1263–1268, 1263-1268.
Westedt, U., Kalinowski, M., Wittmar, M., Merdan, T., Unger, F., Fuchs, J., Schüler, S., Bakowsky, U., Kissel, T., 2007. Poly(vinyl alcohol)-graft-poly(lactide-co-glycolide) nanoparticles for local delivery of paclitaxel for restenosis treatment. J. Control. Release 119, 41–51.
Wu, J., Liu, Q., Lee, R.J., 2006. A folate receptor-targeted liposomal formulation for paclitaxel. Int. J. Pharm. 316, 148–153.
Xiong, M.P., Yáñez, J.A., Remsberg, C.M., Ohgami, Y., Kwon, G.S., Davies, N.M., Forrest, M.L., 2008. Formulation of a geldanamycin prodrug in mPEG-b-PCL micelles greatly enhances tolerability and pharmacokinetics in rats. J. Control. Release 129, 33–40.
Yadav, A.K., Mishra, P., Mishra, A.K., Mishra, P., Jain, S., Agrawal, G.P., 2007. Development and characterization of hyaluronic acid-anchored PLGA nanoparticulate carriers of doxorubicin. Nanomed: Nanotechnol. Biol. Med. 3, 246–257.
Yigitbasi, O.G., Younes, M.N., Doan, D., Jasser, S.A., Schiff, B.A., Bucana, C.D., Bekele, B.N., Fidler, I.J., Myers, J.N., 2004. Tumor cell and endothelial cell therapy of oral cancer by dual tyrosine kinase receptor blockade. Cancer Res. 64, 7977–7984.
Zhang, X., Jackson, J.K., Burt, H.M., 1996. Development of amphiphilic diblock copolymers as micellar carriers of taxol. Int. J. Pharm. 132, 195–206.
Zhang, X., Li, Y., Chen, X., Wang, X., Xu, X., Liang, Q., Hu, J., Jing, X., 2005. Synthesis and characterization of the paclitaxel/MPEG-PLA block copolymer conjugate. Biomaterials 26, 2121–2128.